Astron. Astrophys. 358, L83–L87 (2000)

ASTRONOMY AND ASTROPHYSICS

LETTER

Letter to the Editor

The ISO spectra of Uranus and Neptune between 2.5 and 4.2 μm: constraints on albedos and H_3^+

Th. Encrenaz[1], **B. Schulz**[2], **P. Drossart**[1], **E. Lellouch**[1], **H. Feuchtgruber**[3], **and S.K. Atreya**[4]

[1] DESPA, Observatoire de Paris, 92195 Meudon, France
[2] ISO Data Center, ESA, PO box 50727, 28080 Madrid, Spain
[3] MPI, Postfach 1603, 85740 Garching, Germany
[4] The University of Michigan, Ann Arbor, MI 48109-1243, USA

Received 31 March 2000 / Accepted 24 May 2000

Abstract. Spectra of Uranus and Neptune were recorded in May 1997, between 2.5 and 4.2 μm, using the ISOPHOT-S instrument. The two planets were detected at 2.75 μm, with geometric albedos of 0.0015 and 0.0052 for Uranus and Neptune respectively. In the case of Uranus, the shape of the CH_4 absorption is consistent with a reflection over the 3 bar-level cloud level, presumably due to H_2S; in the case of Neptune, the reflection seems to take place above the CH_4 cloud at about 0.3 bar. Two ISO-SWS spectra of Uranus, recorded around 3.3 μm in April and May 1998, show the presence of four H_3^+ emission lines. From the May 1998 data, the inferred H_3^+ column density is $0.1 - 40 \times 10^{12}$ cm^{-2}, and the rotational temperature is 600 ± 200 K. The observed H_3^+ emission is significantly stronger than previous ground-based determinations, obtained in 1992 and 1995.

Key words: planets and satellites: general – planets and satellites: individual: – infrared: solar system

1. Introduction

The spectra of Uranus and Neptune between 2.5 and 4.2 μm are expected to be mostly due to reflected sunlight, dominated by strong CH_4 and CH_3D absorptions, except in a window at 2.7 μm which has not been detected so far. Discrete H_3^+ lines, formed in Uranus' thermosphere, have been detected from the ground at 4 μm (Trafton et al., 1993; 1999; Lam et al., 1997).

We present here new spectra of Uranus and Neptune in the 2.5-4.2 μm range, recorded with ISOPHOT-S. Two SWS spectra of Uranus were also recorded around 3.3 μm and show the detection of four H_3^+ emission lines. We analyse below the CH_4 absorptions and the inferred albedos of Uranus and Neptune at 2.75 μm, and we derive the H_3^+ rotational temperature and column density on Uranus.

Send offprint requests to: Th. Encrenaz

2. Observations and data reduction

The photometer ISOPHOT (Lemke et al., 1996) of ISO (Kessler et al., 1996) included a subsystem (PHT-S) consisting of two grating spectrometers operating simultaneously at 2.47 - 4.87 μm (SS) and 5.84 - 11.6 μm (SL), with a spectral resolution of 0.0445 μm and 0.0949 μm respectively (Klaas et al., 1996). The aperture was 24 x 24$''^2$.

PHT-S spectra of Uranus and Neptune were recorded on May 8, 1997. The diameters of Uranus and Neptune were respectively 3.55 and 2.25$''$. In the case of Uranus, four pairs of spectra, with 512 sec integration time per spectrum, were recorded successively on and off the source (with the offset position at 5$'$north), in order to subtract the sky background. In the case of Neptune, twelve of these pairs, with 1024 sec integration time per spectrum, were recorded. The total integration time, including background measurements, was 1.5 hours for Uranus and 6.8 hours for Neptune.

The data reduction up to SRD-level was performed using the PHT Interactive Analysis software package PIA V7.3.2(e) (Gabriel et al., 1997) followed by some proper IDL routines, that facilitate individual inspection of the signals, deglitching and flux calibration. A full description of the data reduction procedure applied to the present PHT-S data can be found in Encrenaz et al. (2000).

Fig. 1 shows the PHT-S spectra of Uranus and Neptune between 2.5 and 4.2 μm. Both planets are unambiguously detected in the 2.75 μm window; Neptune is the weakest source detected with ISOPHOT-S at this wavelength. Beyond 3.5 μm, however, the noise increases significantly, due to systematic effects not included in the error bars. Our conclusion is that, above 3.5 μm, there is no significant flux detection on any of the two planets.

Two ISO-SWS spectra of Uranus were recorded between 3.295 and 3.335 μm, with AOT SWS02 (de Graauw et al., 1996); the spectral resolving power was 1950. The aperture was 14 x 20 $''^2$. The first spectrum was recorded on April 7, 1998 (one day before helium boil off) with an integrated time (on target) of 2694 s, and covered the 3.295 - 3.325 μm range. The second

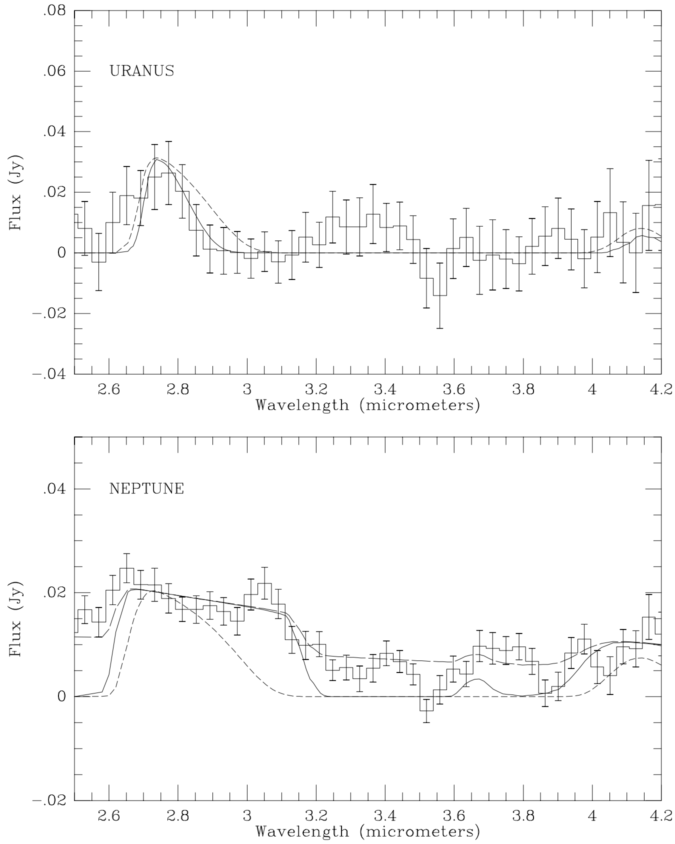

Fig. 1. Histograms: PHT-S spectrum of Uranus (upper part) and Neptune (lower part) observed in the 2.5 - 4.2 μm range. The resolving power (after binning) is about 50. Solid lines (best-fit models): RLM synthetic spectra with [CH_4] = 3.8 km-Am (Uranus) and 0.025 km-Am (Neptune). Dotted lines: synthetic spectra using the parameters of Fink and Larson (1979): [CH_4] = 1.6 km-Am (Uranus) and 0.7 km-Am (Neptune). In the case of Neptune, the dashed-dotted line is the sum of a solar blackbody curve (50%) and the solid-line model (50%).

spectrum was taken on May 9, 1998, when the instrument was significantly warmer; as a result, the wavelength range shifted to 3.310 - 3.334 μm. The on-target time was 1064 s. Data were processed within the SWS interactive analysis system, based on standard ISO pipeline OLP V7.0 products. The data reduction adhered to the recommendations of Salama et al. (1997). The absolute calibration uncertainty around 3.3 μm is a nominal 5% for the April 1998 spectrum and 10% for the May 1998 spectrum.

Fig. 2 shows the observed spectra. The 1-σ noise level is 0.01 Jy. In the first spectrum, three emission lines of the $H_3{}^+$ ν_2 band (Majewski et al., 1987) are detected at 3.3003 μm (3029.82 cm^{-1}), 3.3063 μm (3024.55 cm^{-1}) and 3.3170 μm (3014.25 and 3015.24 cm^{-1}) respectively. The second spectrum shows the same $H_3{}^+$ doublet at 3.3170 μm, with an intensity remarkably similar to the one of the previous observation. Another $H_3{}^+$ line shows up at 3.3255 μm. There is a small shift with respect to the actual central position (3008.11 cm^{-1}, or 3.3243 μm) probably due to the temperature increase of the instrument.

3. Interpretation

3.1. Uranus and Neptune: the 2.75 μm window

It can be seen from Fig. 1 that the albedos of Uranus and Neptune are extremely low. We infer, at 2.75 μm, geometrical albedos of 0.0015 and 0.0052 for Uranus and Neptune respectively, to be compared to 0.3 for Jupiter and 0.15 for Saturn (Encrenaz et al., 1999). In order to understand the origin of these low albedos, we first estimated the possible contribution due to atmospheric gases. We used the slope of the CH_4 absorption band between 2.7 and 3.2 μm to estimate the atmospheric level above which the observed radiation comes from. We used a line-by-line, reflecting-model calculation with an airmass of 3, corresponding to full disk observations. We chose this first-order model to get a qualitative fit of our data, as the moderate S/N of the PHT-S spectra would prevent in any case an accurate determination of the atmospheric parameters. We used the CH_4 databases of GEISA (Jacquinet-Husson et al., 1997), Wenger and Champion (1998) and L. Brown (priv. comm); a total of more than 60000 CH_4 lines were included. For the far wings of CH_4, we used the shape factor derived by Hartmann (priv. comm.) from a laboratory analysis of CH_4 around 3 μm. For each individual line centered at the frequency σ_0, this shape factor is the product of the Lorentz shape factor by a function $\chi(\sigma)$ equal to 1 for (σ-σ_0) lower than 26 cm^{-1}, 8.72 exp[-(σ-σ_0)/12] for (σ-σ_0) between 26 and 60 cm^{-1}, and 0.0684 exp[-(σ-σ_0)/393] for (σ-σ_0) larger than 60 cm^{-1}. Beyond 4 μm, we included the contribution of the CH_3D ν_2 band (Jacquinet-Husson et al., 1987) with a CH_3D/CH_4 ratio of 3.6 10^{-4} for both Uranus (de Bergh et al., 1986) and Neptune (Orton et al., 1992). The rotovibrational fundamental band of the H_2-H_2 collision-induced absorption, centered around 2.3 μm (Birnbaum et al., 1996), was also included in our calculations; absorption due to H_2-He collisions was found to be negligible.

For both Uranus and Neptune, we used the atmospheric structures derived by Baines et al. (1995) and we considered, for each planet, two possible models. In the case of Uranus, the first model assumes the CH_4 column density (1.6 km-Am) inferred by Fink and Larson (1979) from the study of other near-infrared bands. This column density corresponds to a reflection above a pressure level of about 1.5 - 2 bars; we note however that there is no identified cloud layer at this level in Baines et al.'s model. The second model assumes a reflection above a thick cloud, possibly due to H_2S, located at 3.13 bars (Baines et al., 1995); the CH_4 column density is then 3.8 km-Am. It can be seen from Fig. 1 that the PHT-S data favor the second model, in agreement with the conclusions derived by Baines et al. (1995) from a study of the visible and near-IR methane bands.

In the case of Neptune, our first model uses a CH_4 column density of 0.7 km-Am, following the results of Fink and Larson (1979); our second model assumes a reflection at a much higher level, above the top of the CH_4 cloud level at 0.34 bar. Assuming a CH_4 mixing ratio of 7 10^{-4} above this level (Bézard, 1998), we derive a methane column density of 0.025 km-Am. As shown in Fig. 1, the latter model provides a better agreement to the ISO data. We conclude that the 2.7 μm radiation

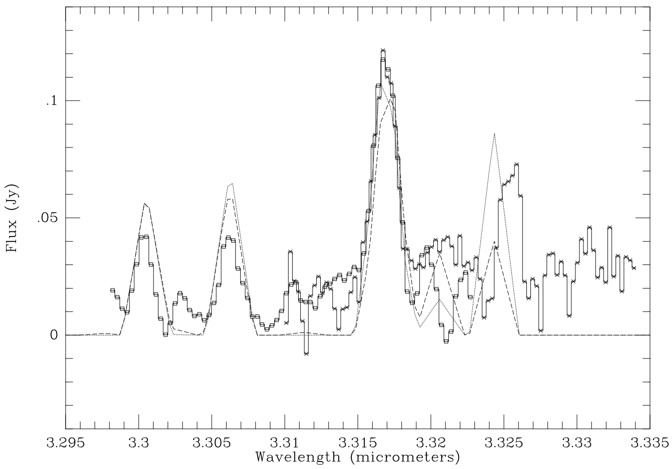

Fig. 2. The SWS spectra of Uranus in the 3.31 μm region (histograms). Left side (open squares): April 7, 1998; right side (crosses): May 9, 1998. Four emission lines of H_3^+ are detected. The wavelength mismatch at 3.325 μm is attributed to the temperature increase of the instrument one month after helium boil off. The ISO data are compared to two synthetic spectra, normalized at 3.317 μm, corresponding to temperatures of 400 K (dotted line) and 1000 K (dashed line).

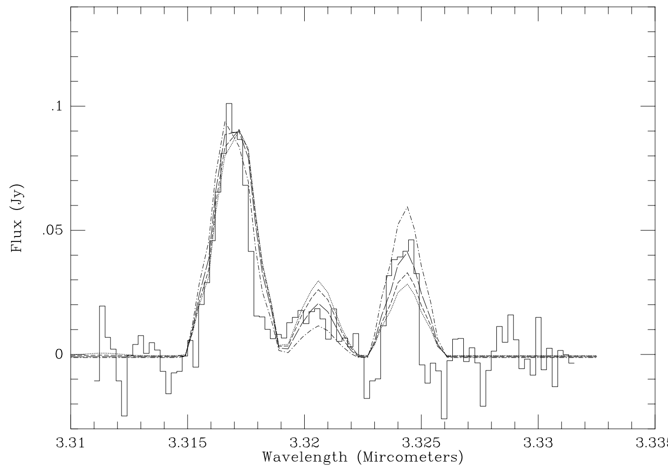

Fig. 3. The SWS spectrum of 9 May 1998 (histograms) compared to four synthetic spectra normalized at 3.317 μm. From top to bottom at 3.325 μm: T = 400 K, 600 K, 800 K, 1000 K.

is likely to be reflected or scattered from above the top of the CH_4 cloud. Fig. 1 also suggests that this better fit is improved if some contribution of solar continuum is added. This component would be consistent with 50% of the flux being reflected at a higher altitude, presumably the hydrocarbon haze around 0.01 bar (Baines et al., 1995). We note that, for both Uranus ad Neptune, our results differ from the ones of Fink and Larson (1979), but are consistent with the models of Baines et al. (1995).

Using the models derived above, we estimate, for the albedos of Uranus and Neptune at 2.75 μm, the contribution due to CH_4 and H_2 absorptions. At this wavelength, the transmission due to CH_4 is found to be 0.5 for Uranus and 1.0 for Neptune; the transmission due to H_2 is also 0.5 for Uranus and 1.0 for Neptune. As a result, the albedos of Uranus and Neptune, without the gaseous contribution, are respectively 0.0060 and 0.0052.

The origin of these low albedos remains to be understood. The strong absorption might be due to solid particles, either in a haze (possible hydrocarbon condensates, or photochemistry/irradiation products) or at the cloud level. There is indeed a band of H_2S ice located around 2.7 μm, but this band is weak and narrow (0.01 μm at 107 K; Schmitt, priv. comm.) The higher albedo of Neptune at 2.75 μm, as compared to the Uranus value, might come from a reflection over discrete CH_4 cirrus which are known to cover only a small fraction of the disk, with possibly an additional component reflected at higher levels. Assuming a typical albedo of 0.5 for these clouds, we infer that, at first order, the flux of Neptune could be explained by the sum of a ”Uranus-type” spectrum reflected at deep levels with an albedo of 0.0015, a contribution of cirrus clouds, of albedo 0.5, covering about 0.4% of the Neptune disk and thus contributing to 0.0020 of the total albedo, and a high-altitude reflected component also contributing to 0.0020. The fraction of CH_4 cirrus is roughly compatible with the Voyager images; however this quantity is known to be variable, as shown by previous ground-based and HST observations (Hammel and Lockwood, 1997).

3.2. *The H_3^+ emission spectrum of Uranus*

Fig. 2 shows the SWS spectra of Uranus compared to synthetic spectra at two rotational temperatures, 400 K and 1000 K. H_3^+ lines originate from the thermosphere, at pressures lower than a μbar. The H_3^+ column densities were calculated using a radiative transfer model through optically thin layers (Drossart et al., 1993). The column densities corresponding to 400 and 1000 K are 3.7×10^{13} cm^{-2} and 3.8×10^{10} cm^{-2}, respectively.

Fig. 2 shows that the relative intensities of the three H_3^+ lines observed in the April 1998 spectrum (at 3.300, 3.306 and 3.317 μm) show no temperature sensitivity. Their fit with the data is not quite satisfactory, which might be due to a poor determination of the continuum level. In contrast, it can be seen from Fig. 2 that both the 3.325 μm line and the undetected weaker line at 3.321 μm exhibit some temperature sensitivity. We have used the May 1998 spectrum, after correcting its wavelength scale and removing its residual continuum slope, to estimate the H_3^+ rotational temperature. The result, as shown in Fig. 3, is T = 600 ± 200 K. The corresponding H_3^+ column density is 7×10^{11} cm^{-2}, with a very large uncertainty range ($0.1 - 40 \times 10^{12}$). The similarity of the two SWS spectra in the 3.317 μm H_3^+ line suggests that the H_3^+ parameters were similar in April and May 1998.

From previous observations at 4.0 μm, rotational temperatures of 740 K (April 1992; Trafton et al., 1993) and 680 K (June 1995; Lam et al., 1997) were measured, corresponding to H_3^+ column densities of 6.5×10^{10} and 5.3×10^{10} cm^{-2} respectively. The temperature measurements were confirmed by Trafton et al. (1999) who updated and completed these results (Table 6 of their paper). Our determination of the temperature, which is actually quite uncertain, is compatible with their results, but our H_3^+ column density is significantly larger. In any

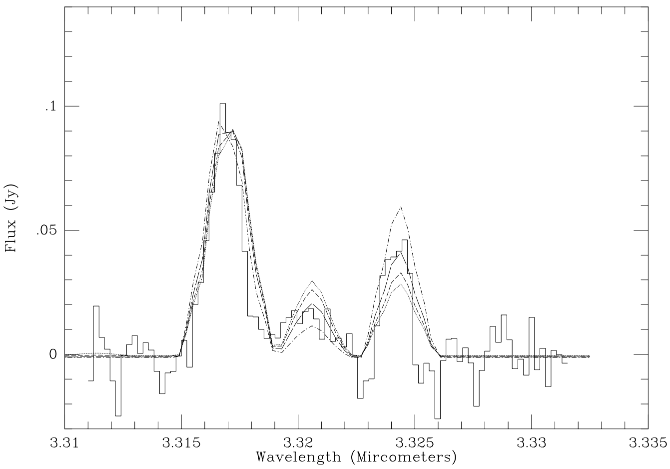

Fig. 4. The PHT-S spectrum of Uranus (histograms) compared to two synthetic $H_3{}^+$ spectra, normalized to the SWS value at 3.31 μm (convolved to the PHT-S resolution), corresponding to T = 400 K (solid line) and T = 1000 K (dashed line). We note that there is no contribution from $H_3{}^+$ in the 2.75 μm window.

case, the $H_3{}^+$ emission observed by ISO is stronger than previous measurements.

As the $H_3{}^+$ ν_2 emission is maximum in the region of 4 μm, we have searched for a possible contribution of $H_3{}^+$ in our PHT-S spectrum. We extended the synthetic spectrum of $H_3{}^+$ up to 4.2 μm and, as a working hypothesis, we normalized it to the SWS observed value at 3.31 μm, after convolution to the PHT-S spectral resolution (i.e. assuming the same $H_3{}^+$ emission in May 1997 and May 1998). The result is shown in Fig. 4. It can be seen that this $H_3{}^+$ contribution slightly improves the fit between 3.0 and 3.5 μm. However, if this $H_3{}^+$ contribution were real, the absence of flux at 4 μm, in the PHT-S spectrum of Uranus, would imply a temperature as high as 1000 K, i. e. higher than our May 1998 value. A more plausible explanation is that there is no signal detected at 3.0 - 3.5 μm; in this case, the $H_3{}^+$ parameters derived from SWS for May 1998 are upper limits for the May 1997 observations.

In order to understand the long-term variability of the $H_3{}^+$ emission, it is instructive to review the source of this species in the atmospheres of the giant planets, in general, and Uranus, in particular. $H_3{}^+$ is produced mainly upon a reaction between H_2 and $H_2{}^+$ on these planets, i.e.

$H_2 + H_2{}^+ \rightarrow H_3{}^+ + H$ (R1)

followed by its loss,

$H_3{}^+ + e \rightarrow H + H + H$ (R2)

or

$H_3{}^+ + e \rightarrow H_2 + H$ (R3)

The balance between the production and loss rates determines the profile, hence the column density of $H_3{}^+$ (Atreya, 1986). The observed $H_3{}^+$ emission is related to the density.

The factors affecting the $H_2{}^+$ production vary from Jupiter to Uranus. The solar EUV always ionizes H_2 to produce $H_2{}^+$. However, ionization due to the precipitating magnetospheric charged particles is an additional source. On Jupiter, this ”auroral” $H_3{}^+$ dominates the total planetary $H_3{}^+$ emission (Drossart et al, 1989). On the other hand, on Uranus, whose magnetospheric power input is at least a factor 100 smaller than Jupiter's (Atreya, 1986), the auroral source may account for no more than 20 percent enhancement of the planetary $H_3{}^+$ emission, according to Lam et al (1997). This idea seems to be borne out by an examination of the temporal variability of the $H_3{}^+$ emission. After applying calibration and other corrections to the pre-ISO data, Trafton et al.(1999) summarize in their Table 9 the average integrated $H_3{}^+$ intensities and luminosities from 1992 to 1995. They note a decreasing trend in $H_3{}^+$ from 1992 (very high solar activity) to 1995 (near solar minimum), and find the solar variability of the EUV responsible for such a trend.

The ISO data of May 1997 and April/May 1998 presented here support the trend seen in the $H_3{}^+$ emission intensity reported in Trafton et al. (1999). The ISO observations were done close to the solar maximum, and, in fact, show $H_3{}^+$ emission greater than the ones in the 1995 solar minimum period. It is puzzling, however, that the 1998 $H_3{}^+$ emission intensity is even greater than the one in 1992, while both these observations were carried out near the solar maximum. Of course, the solar ionizing flux, particularly at the very short wavelength, can have extreme variability from one solar maximum epoch to another. Also, the situation is somewhat complicated (and perhaps even aided) by the presence of an H-corona around Uranus, which would absorb a fraction of the solar EUV responsible for ionizing the H_2. The distribution and opacity of the H-corona could be affected not only by the variations in the solar UV (which dissociates the atmospheric H_2) but also the magnetospheric-atmospheric coupling processes. In summary, although the correlation between the $H_3{}^+$ emission and the solar EUV appears to be an attractive and strong possibility, the ISO data demonstrate the situation may be more complicated. Additional observations and modeling will be necessary to resolve this important planetary phenomenon.

Acknowledgements. We thank L. Brown, J.-M. Hartmann and B. Schmitt for giving us access to unpublished laboratory data. We are grateful to L. Trafton for helpful comments regarding this paper.

References

Atreya, S. K. ”Atmospheres and Ionospheres of the Outer Planets and their Satellites”, Springer-Verlag, New York-Berlin, 1986 (chapt. 6).

Baines, K. H., Mickelson, M. E., Larson, L. E., Ferguson, D. W., 1995, Icarus 114, 328

Bézard, B., 1998, Ann. Geophys.16 (Suppl. III), C1037

Birnbaum, G., Borysow, A., Orton, G. S., 1996, Icarus 123, 4

de Bergh, C., Lutz, B., Owen, T., Brault, J., Chauville, J., 1986, ApJ 311, 501

de Graauw, Th., Haser, L. N., Beintema, D. A. et al., 1996, A & A 315, L49

Drossart, P., Maillard, J.-P., Caldwell, J. et. al., 1989, Nature 340, 539

Drossart, P., Bézard, B., Atreya, S. K., Bishop, J., Waite, J. H., Boice, D., 1993, J. Geophys. Res. 98E, 18803

Encrenaz, Th., Drossart, P., Feuchtgruber, H. et al., 1999, Plan. Space Sci. 47, 1225

Encrenaz, Th., Schulz, B., Drossart, P., Lellouch, E., Feuchtgruber, H., Atreya, S. K., 2000, ESA SP-456, in press

Fink, U., Larson, H. P., 1979, ApJ 233, 1021
Gabriel, C. et al., 1997 Proc. of the ADASS VI conference, ASP Conf.Ser., Vol.125, eds. G. Hunt & H.E. Payne, p.108
Hammel, H. B., Lockwood, G. W., 1997, Icarus 129, 466
Jacquinet-Husson N., et al., 1997, JQSRT 62, 205
Kessler, M. F., Steinz, J. A., Anderegg, M. E. et al., 1996, A & A 315, L27
Klaas, U., Acosta-Pulido, J. A., Abraham, P. et al., 1997, ESA SP-419, 113
Lam, H A., Miller, S., Joseph, R. D. et al., 1997, ApJ 474, L73
Lemke, D., Klaas, U., Abolins, J. et al., 1996 A & A, 315, L64
Majewski, W. A., Marshall, M. D., Mc Kellar, A. R. W., Johns, J. W. C., Watson, J. K. G., 1987, J. Mol. Spec. 122, 341
Orton, G. S., Lacy, J. H., Achtermann, J. M., Parmar, P., Blass, W. E., 1992, Icarus 100, 541
Salama, A., Feuchtgruber, H., Heras, A. et al., 1997, ESA SP-419, 17
Trafton, L. M., Geballe, T. R., Miller, S., Tennyson, J., Ballester, G. E., 1993, ApJ 405, 761
Trafton, L., Miller, S., Geballe, T. R., Tennyson, J., Ballester, G. E., 1999, Astrophys. J. 524, 1059
Wenger, Ch., Champion, J.-P., 1998, J. Quant. Spectr. Rad. Transfer 59, 471

LETTER